Published in final edited form as:
Magn Reson Med. 2010 December ; 64(6): 1821–1826. doi:10.1002/mrm.22551.

Use of a Reference Tissue and Blood Vessel to Measure the Arterial Input Function in DCEMRI

Xiaobing Fan, **Chad R. Haney**, **Devkumar Mustafi**, **Cheng Yang**, **Marta Zamora**, **Erica J. Markiewicz**, and **Gregory S. Karczmar***
Department of Radiology, The University of Chicago, Chicago, Illinois, USA

Abstract

Accurate measurement of the arterial input function is critical for quantitative evaluation of dynamic contrast enhanced magnetic resonance imaging data. Use of the reference tissue method to derive a local arterial input function avoided large errors associated with direct arterial measurements, but relied on literature values for K^{trans} and v_e. We demonstrate that accurate values of K^{trans} and v_e in a reference tissue can be measured by comparing contrast media concentration in a reference tissue to plasma concentrations measured directly in a local artery after the 1–2 passes of the contrast media bolus—when plasma concentration is low and can be measured accurately. The values of K^{trans} and v_e calculated for the reference tissue can then be used to derive a more complete arterial input function including the first pass of the contrast bolus. This new approach was demonstrated using dynamic contrast enhanced magnetic resonance imaging data from rodent hind limb. Values obtained for K^{trans} and v_e in muscle, and the shape and amplitude of the derived arterial input function are consistent with published results.

Keywords

dynamic contrast enhanced MRI; arterial input function; pharmacokinetic model; volume transfer constant of contrast agent

INTRODUCTION

Dynamic contrast enhanced magnetic resonance imaging (DCEMRI) plays an important role in clinical detection and diagnosis of cancers (1,2). The pharmacokinetic model that is often used to analyze DCEMRI data (3) requires knowledge of the arterial input function (AIF), which accounts for variations in contrast media injection, cardiac output, and vascular function (4). The AIF can be determined from a major artery (5), a predefined “population” function (6), or a reference tissue (7). However, the direct measurements from arteries are subject to significant systematic errors due to the very high contrast agent concentration at early times after injection, partial volume effects, and in-flow affects (8,9). The “population” AIF does not account for significant variability between patients and contrast media injections. To avoid these problems, “reference tissue methods” (7,10,11) were developed to infer the AIF from measurements of contrast media concentration versus time in normal tissue with known physiological properties. Reference tissue methods do not require measurements of high contrast media concentration in an artery. They provide high signal-to-noise ratio (SNR) because a large volume of relatively homogeneous normal tissue can be used, and they provide a local AIF for each subject, since a reference tissue close to the

*Correspondence to: Gregory Karczmar, Department of Radiology, MC2026, University of Chicago, 5841 S. Maryland Ave., Chicago, IL 60637. gskarczm@uchicago.edu.

cancer can be selected. The original "reference tissue method" (7) relied on the literature values for the volume transfer constant (K^{trans}) and the contrast media distribution volume (v_e) as a starting point, and these may differ significantly from the true value for each experimental subject. Recently, a more accurate reference tissue method has been developed to determine a consensus AIF based on contrast media dynamics in two (10,11) or more reference tissues (12). The newer method is more robust, but accurate calculation of K^{trans} and v_e in the reference tissues is not guaranteed, and there is still a possibility for systematic error. The multiple reference tissue approach requires a literature value of v_e from one reference tissue to scale the AIF, and the true value for v_e may be significantly different from the literature value.

Here we introduce a new method to more accurately determine K^{trans} and v_e for a reference tissue, and thereafter to derive the entire AIF more accurately. The approach assumes that (i) the contrast concentration in an artery can be measured accurately by MRI after the first 1–2 passes of the contrast media bolus (about 30–60 seconds after injection in rats) when the plasma concentration of contrast media is low and changes slowly; (ii) contrast media dynamics in a reference tissue (e.g., muscle) can be accurately described by a simple physiological model, e.g., the two compartment model with or without a vascular term; (iii) contrast media concentration in plasma and in a reference tissue with modest perfusion are far from equilibrium for several minutes after injection. The latter assumption is supported by simulations based on published models for the AIF, K^{trans} and v_e, and is also consistent with the experimental data presented here (e.g., please see Fig. 3 and the accompanying discussion). With these assumptions, the difference between the plasma and reference tissue concentrations of contrast media over time can be analyzed to derive K^{trans} and v_e for the reference tissue (see "Materials and Methods" section). In the following, we refer to this new approach as the "RTPV" (reference tissue plus vessel) method. The RTPV is illustrated using preclinical DCEMRI data acquired from the hind limbs of rats.

MATERIALS AND METHODS

This was a retrospective study, based on data acquired from Copenhagen rats with AT6.1 metastatic prostate tumors in the hind limb. However, the analysis described here uses data only from normal skeletal muscle of the hind limb. Data from the tumors was not used in the present study.

MRI Experiments

All surgical procedures were performed in accordance with the University of Chicago Institutional Animal Care and Use Committee guidelines. Animals were anesthetized using Isoflurane gas (~2%) mixed with medical air (2 L/min) and oxygen (0.2 L/min) flowing through a mask. All animals were monitored for heart rate, respiration rate, blood pressure, and temperature using an SA Instruments system (Stony Brook, NY) developed for *in vivo* MRI. Temperature was controlled by blowing warm air through the bore of the magnet. A 24 gauge angiocatheter was placed in the tail veins of the rats for contrast agent injection.

MRI experiments were performed on a 33 cm, horizontal bore, 4.7 Tesla scanner with a Bruker console (Bruker-Biospin, Billerica, MA) equipped with a 20 cm shielded gradient set with a maximum strength of 200 mT/m. The tumor-bearing leg was placed in a Helmholtz coil, 3.0 cm in both diameter and length. For DCEMRI experiments, the middle three slices covering the largest cross-sectional area of tumor were selected along the long axis of the leg. T_1-weighted gradient echo images (TR/TE = 40/5 msec, field of view = 40 mm × 40 mm, matrix size = 128 × 128, slice thickness = 1.0 mm, flip angle = 30°, number of averages = 1) were acquired with 5 sec temporal resolution for the first ~10 min after contrast media injection, and subsequently with ~10 sec temporal resolution for another ~10 min. There

was a ~7 min gap between first and second set of DCEMRI data while other MRI data (not used in this study) were acquired. The contrast agent, Gadodiamide (OmniScan®, GE Healthcare, Piscataway, NJ), was injected ~30 sec after the start of the acquisition at a typical dose of 0.2 mmol/kg of body weight (0.2 mL of 95.7 mg/mL of OMNISCAN in saline) over ~5 sec.

Estimation of K^{trans} and v_e

Contrast media concentration as a function of time [$C(t)$] was determined from signal intensity using a previously published method (13). Then DCEMRI data were analyzed using the following protocol to estimate K^{trans} and v_e for a reference tissue (skeletal muscle):

Step 1: Determine AIF—Small arteries in the leg were selected to determine plasma concentration of contrast media. The velocity of blood flow in these small vessels is much lower than in the aorta (14) and flow was primarily in the plane of the imaged slice. Therefore, in-flow effects were expected to be modest, so that contrast media concentration could be accurately measured from MRI signal intensity, after the first one or two passes of the bolus. Contrast concentration as a function of time from the vessel, $C_a(t)$, was measured in a single candidate pixel to minimize the partial volume effects. The portion of the curve after the apparent peak (t_{peak}) enhancement was fitted by bi-exponential function $a_0 \cdot \exp(-m_0 t) + a_1 \cdot \exp(-m_1 t)$, and compared with published values determined by MRI measurements of the arterial plasma contrast media concentration in rats' tails (15). Pixels in the blood vessel were tested until a fit for $C_a(t)$ with parameters near the previously published results were found. This insured that the selected pixel was in an artery. The acceptable ratio for "a_0/a_1" was from 1.5 to 3.0, and the acceptable ratio for "m_0/m_1" was from 28.0 to 79.0. These acceptable ratio ranges were calculated from the values listed in Table 2 of reference 15. Data from the selected pixel in the blood vessel was used for subsequent calculations. Measurements of $C_a(t)$ were considered to be an accurate measure of the AIF at times greater than t_{peak}, when contrast media concentration in the artery was generally less than 1 mM, i.e., low enough to minimize T_2^* effects and effects of water exchange across red cell membranes. Note that the measured t_{peak} is not the true peak of the arterial concentration. The true peak is generally missed due to limited temporal resolution and errors caused by high plasma concentrations of contrast media. Finally, $C_a(t)$ was corrected using published values for the average arterial hematocrit in the rat (Hct = 0.45) (5) to define $\hat{C}_p(t) = C_a(t)/(1\text{-Hct})$ as the plasma AIF in the leg.

Step 2: Measure $C_m(t)$ in the Reference Tissue—The contrast media concentration as a function of time, $C_m(t)$, was obtained from a region of interest (ROI) with 9 × 9 pixels in a portion of the leg muscle away from the tumor with relatively uniform contrast media uptake. To moderate the effect of noise, the curve was fitted using a previously published empirical mathematical model (EMM) (16), and the EMM fit was used in the remaining calculations. Specifically, the muscle curves were fitted by the following equation:

$$C_m(t) = A \cdot (1 - \exp(-\alpha t))^q \cdot \exp(-\beta t) \cdot (1+\exp(-\gamma t))/2,$$

where A is the upper limit of the tracer concentration, α (min^{-1}) is the rate of uptake, β (min^{-1}) is the overall rate of washout, γ (min^{-1}) is the initial rate of washout, and q is related to the slope of uptake.

Step 3: Estimate v_e for $C_m(t)$—The slope of $C_m(t)$ was close to 0 at time $t \geq$ ~30 min. This can be seen from the EMM parameters for the muscle curve at $t \geq$ ~30 min, i.e., $|dC_m(t)/dt| < |A\beta|$, which is a very small number. Therefore, we assumed that the interstitial

and venous plasma tracer concentrations were very close to equilibrium at a late time (~30 min) after a bolus of contrast injection. Under this equilibrium condition, we have the following relation:

$$\widehat{C}_{\mathrm{p}}(t)=C_{\mathrm{m}}(t)/v_{\mathrm{e}} \rightarrow v_{\mathrm{e}}=C_{\mathrm{m}}(t)/\widehat{C}_{\mathrm{p}}(t) \text{ at } t \geq \sim 30 \text{ min}.$$

Step 4: To Estimate K^{trans} From $C_m(t)$—We assumed that the muscle was well approximated by the two compartment model (TCM):

$$\frac{dC_{\mathrm{m}}(t)}{dt}=K^{\mathrm{trans}}(C_{\mathrm{p}}(t)-C_{\mathrm{m}}(t)/v_{\mathrm{e}}), \quad [1]$$

where $C_p(t)$ is the AIF. From Eq. 1, the regional AIF [$C_p(t)$] can be calculated from $C_m(t)$ in muscle, i.e.,

$$C_{\mathrm{p}}(t)=\frac{1}{\mathrm{K}^{\mathrm{trans}}}\frac{dC_{\mathrm{m}}(t)}{dt}+\frac{C_{\mathrm{m}}(t)}{v_{\mathrm{e}}}, \quad [2]$$

where v_e was determined in Step 3. To estimate K^{trans} in muscle, K^{trans} values in Eq. 2 were searched between 0.001 and 0.5 min^{-1} by using the "golden section" method to find the best fit for the measured $\hat{C}_p(t)$ for times greater than t_{peak} but less than 5 min. Finally, from estimated values for K^{trans} and v_e determined from from Steps 1–4, the complete AIF beginning at $t = 0$ was calculated from Eq. 2. Note that an accurate value for K^{trans} can be determined from Eq. 2 only if the difference between $\hat{C}_p(t)$ and $C_m(t)/v_e$ is much greater than the noise. Therefore, the optimal reference tissue for this approach has a relatively low K^{trans}, so that contrast agent concentrations in the plasma and reference tissue approach equilibrium slowly.

RESULTS

Figure 1 shows a typical image and plots of contrast media concentration in muscle and in the local artery to illustrate the steps followed for estimating K^{trans} and v_e in the muscle ROI. Figure 1a shows $\hat{C}_p(t)$ (gray dots) measured from the selected blood vessel pixel (indicated by an arrow in image) and the best fit bi-exponential function for times greater than t_{peak} (purple line). Please notice that the fitted line was extrapolated back to zero from the t_{peak}. Due to the ~5 sec temporal resolution and high contrast concentration at the peak of the bolus, the true peak of $\hat{C}_p(t)$ was missed and only the portion of the curve after the measured peak ($t \geq t_{peak}$) could be accurately determined from MRI. The bi-exponential fit was excellent in spite of the gap in the data and the parameters were within the range of published results for arteries in rats. The $C_m(t)$ (Fig. 1b open square) for the muscle ROI (indicated by square in image) was accurately fitted by the EMM (blue line). In this example, based on the EMM fit to $C_m(t)$ and the bi-exponential fit to $\hat{C}_p(t)$, we obtained values for K^{trans} and v_e of 0.12 min^{-1} and 0.19, respectively.

Figure 1c shows the complete AIF (red line) derived from using the estimated K^{trans} and v_e in the reference ROI. The derived AIF accurately fits the measured $\hat{C}_p(t)$ (gray dots) for times greater than t_{peak}. However, the derived AIF does not match the early portion of $\hat{C}_p(t)$, and has a much higher maximum amplitude.

The same procedure (above) was applied to analyze data from eight experiments. The parameters for the bi-exponential fits to the $\hat{C}_p(t)$, the EMM fits to $C_m(t)$, and estimated K^{trans} and v_e for muscle are given in Table 1. For the bi-exponential fits to the $\hat{C}_p(t)$ curves, the ratio of a_0/a_1 was in the range of 1.6–3.2, and ratio of m_0/m_1 was in the range of 29.0–44.0. Thus, our bi-exponential fitting parameters are within the range of previously published values (15). The directly measured average peak SNR for vessel and muscle were 41 ± 10 and 10 ± 3, respectively. The average values of K^{trans} and v_e for all eight cases were 0.14 ± 0.06 (min^{-1}) and 0.19 ± 0.05, respectively. Figure 2 shows average curves (thick gray lines) over eight cases for (a) bi-exponential fits to the AIF, (b) EMM fits for $C_m(t)$, and (c) the AIF derived from the estimated K^{trans} and v_e using the reference tissue method. The thin black lines show the standard deviation of the distributions at each time point - demonstrating significant variability within the group. The peak amplitude of the AIF derived using the reference tissue was 2.77 ± 1.19 mM, and the peak amplitude of $\hat{C}_p(t)$ measured directly from the vessel was 0.69 ± 0.07 mM. This difference was statistically significant ($P < 0.002$).

Figure 3 shows plots of $\hat{C}_p(t)$ and $C_m(t)/v_e$ that were generated using typical parameters from Table 1 (Cases 2 and 3). For Case 2, the plasma concentration of contrast media is higher than the muscle concentration until ~90 seconds after bolus arrival. After the muscle and plasma curves cross, the plasma concentration drops well below muscle, because the washout of contrast from muscle (with a rate constant of ~0.3 min^{-1}) cannot keep up with the washout from plasma (with a rate constant of ~0.5 min^{-1}). For Case 3, the plasma concentration of contrast media remains above the extracellular concentration in muscle for over 2 minutes. In general in the rat hind limb, there is a 2–10 minute period when there is a significant concentration difference (positive or negative) between muscle and plasma that can be measured with adequate SNR (Fig. 3), so that K^{trans} can be accurately measured.

DISCUSSION

The results demonstrate that K^{trans} and v_e can be calculated from contrast media concentrations in a reference tissue with modest blood flow and an artery, using data acquired after the end of the first pass of the contrast agent bolus. At these times, the plasma concentration is relatively low and is changing slowly. Therefore, it can be measured accurately with high spatial resolution and SNR, if in-flow effects are minor, or accounted for. As long as the difference between concentrations of contrast media in the extracellular space of the reference tissue and the arterial plasma is significantly greater than the noise level, the reference tissue K^{trans} and v_e can be estimated from the change in the difference over time.

The contrast media concentration vs. time curve shapes measured directly from small arteries are similar to those obtained by McIntyre et al. (15) from rat tail arteries, and by Weidensteiner et al. (17) from rat jugular veins. However, our curves have lower amplitude; this could be due to dispersion of the AIF in the small vessels we sampled, as well as partial volume effects. The AIFs derived using the RTPV approach are similar in terms of amplitude and shape to the AIFs measured by McGrath et al. (5) in the rat left ventricle using an MRI “semi-keyhole” technique. However they are quite different from the AIFs measured by Yankeelov et al. (18) in rat aorta, based on a combination of blood sampling (at later times after injection) and MRI measurements of phase-shifts caused by the contrast agent during the first pass of the contrast agent bolus.

The AIF measured using the RTPV approach has a much larger peak value than the AIF measured directly from plasma in the same experiment. This is consistent with previous results of Yang et al.—comparing the AIF derived using the “multiple reference tissue

method" with directly measured AIFs (12). The amplitude of the AIF measured directly from an artery is expected to be much lower than the true AIF because of the systematic errors associated with measurement of high concentrations of contrast media [including decreases in T_2^*, and effects of the relatively slow exchange of water between the cytoplasm of red blood cells and the extracellular space (19)], and inadequate temporal resolution (18).

There was considerable variability in the amplitudes and shapes of AIFs measured directly from the vessel and AIFs calculated using the reference tissue. For example, the peak amplitude of the AIFs directly measured from arteries was an average of 0.69 ± 0.07 mM, and the peak amplitude of the AIF's derived from the reference tissue was 2.77 ± 1.19 mM. This variability in both the directly and indirectly measured AIFs demonstrates the value of measuring the AIF on a case-by-case basis. "Population" AIF's are frequently used (20) as input to physiological models, and this approach has important benefits, but cannot account for the range of AIF's observed experimentally.

The average K^{trans} (0.14 ± 0.06 min^{-1}) and v_e (0.19 ± 0.05) values for normal rat hind limb muscle reported here are close to values obtained for rat hypoglossus and masseter muscle (K^{trans} = 0.15 min^{-1} and v_e = 0.2) by Yankeelov et al. (19). However, these values are much larger than rat hind flank muscle K^{trans} and v_e values obtained by Yankeelov et al. (18). This could be due to differences in the acquisition parameters, the shape of AIFs and the muscle groups selected for analysis. Evelhoch (21) demonstrated that contrast injection duration and image acquisition parameters significantly impact the measured kinetics of contrast media uptake and washout, and this in turn affects calculations of K^{trans} and v_e.

Although the K^{trans} and v_e values for muscle estimated using the RTPV method were within the range of literature values (22), there were significant variations across eight experiments. K^{trans} varied by over a factor of four, and v_e varied by more than a factor of two. This demonstrates the importance of calculating individual K^{trans} and v_e values for each experiment, rather than using literature values, as in the original reference tissue method (7).

In the present work, the primary assumption required by the RTPV approach was that contrast dynamics in the reference tissue are well approximated by the two-compartment model, and this assumption is well justified for muscle (7). Other models could be used for other reference tissues, including models that explicitly include the blood compartment; the only requirement is that the model reliably and accurately represents contrast media dynamics in the reference tissue.

The RTPV method eliminates systematic errors due to differences between the true K^{trans} and v_e and literature values. However, new sources of measurement errors are introduced. One source of error is the modest sensitivity of the reference tissue to very rapid changes in the plasma concentration of contrast media (e.g., during the first pass of the contrast agent bolus). A reference tissue with low K^{trans} is desirable, because it comes to equilibrium with the plasma slowly. However, this also reduces sensitivity to high frequency components of the AIF, since K^{trans} determines the response of tissue to changes in plasma contrast media concentration, especially during the first pass. In principle even a reference tissue with low K^{trans} can be used to detect high frequency components of the AIF if the SNR is very high, but low SNR and K^{trans} in combination will produce significant errors in the calculated AIF. The variance associated with use of a specific reference tissue and blood vessel depends on many factors including the true AIF, the K^{trans} and v_e of the reference tissue, the SNR, and the degree of T1-weighting. A complete treatment of sources of error will require simulations and this work is currently in progress.

The “in-flow” effects are an additional source of error. When plasma concentrations of contrast media are measured directly from the aorta, rapid flow of blood perpendicular to the imaged slice can cause large errors in the calculation of contrast media concentration (9). In the experiments discussed here, a small artery was used for concentration measurements. Flow in these smaller vessels is significantly slower than in the aorta, and in addition, the portion of each vessel selected was in the plane of the imaged slice. Therefore, in-flow effects were probably modest. The values of v_e, calculated by comparing $C_m(t)$ to $\hat{C}_p(t)$, were within the normal range; this is an indication that the correct values for $\hat{C}_p(t)$ were measured. Nevertheless, measurements that account for in-flow effects would increase accuracy (9). In addition, in-flow effects could be decreased by acquiring 3D images from thick slabs, as opposed to the multislice protocol used here (23).

Although the relatively slow blood flow to the reference tissue is a potential weakness of the RTPV method, this problem could be avoided. Once K^{trans} and v_e for the “slow flow” reference tissue are known, K^{trans} and v_e for a reference tissue with more rapid blood flow can be calculated. This would be a special case of the double reference tissue method, the multiple reference tissue developed by Yang et al. (12), and the multiple region method of Yankeelov et al. (11), in which K^{trans} and v_e for the slower reference tissue would be fixed (or allowed to vary only within a small range), based on the calculations described here using the RTPV method. Then the reference tissue with high K^{trans} can be used to further improve AIF estimation, particularly at early times after injection.

The RTPV approach requires accurate measurement of the contrast media washout from a local artery. There may be cases where no artery is available or where partial volume effects are significant. However, in general, scans can be prescribed to include arteries of adequate size. As is always the case with reference tissue methods, it is preferable to select reference tissues that are close to the area to be studied (e.g., a tumor) so that a local AIF can be measured. However, previous work from this group demonstrated that impulse response analysis can refine any AIF so that it more accurately reflects local properties (24).

In summary, an improved reference tissue approach for measuring the AIF in DCEMRI has been demonstrated. The K^{trans} and v_e estimated for the muscle reference tissue were close to the literature values. The AIFs derived based on $C_m(t)$ were close to published AIF’s for rats. The proposed method is a significant improvement relative to the original reference tissue method (7) and may offer advantages relative to later variants of the reference tissue method (11,12). The RTPV method has the potential to significantly reduce the systematic error in parameters calculated from DCEMRI data, and thus increase diagnostic accuracy and sensitivity to drug effects. Future studies with patient data and simulations will be performed to validate the technique and evaluate its limitations.

Acknowledgments

NIH; Grant number: R33CA100996-02; Grant sponsor: SPORE; Grant number: P50 CA125183-01

References

1. Radjenovic A, Dall BJ, Ridgway JP, Smith MA. Measurement of pharmacokinetic parameters in histologically graded invasive breast tumours using dynamic contrast-enhanced MRI. Br J Radiol. 2008; 81:120–128. [PubMed: 18070824]
2. Bonekamp D, Macura KJ. Dynamic contrast-enhanced magnetic resonance imaging in the evaluation of the prostate. Top Magn Reson Imaging. 2008; 19:273–284. [PubMed: 19512849]
3. Armitage P, Behrenbruch C, Brady M, Moore N. Extracting and visualizing physiological parameters using dynamic contrast-enhanced magnetic resonance imaging of the breast. Med Image Anal. 2005; 9:315–329. [PubMed: 15950895]

4. Port RE, Knopp MV, Brix G. Dynamic contrast-enhanced MRI using Gd-DTPA: interindividual variability of the arterial input function and consequences for the assessment of kinetics in tumors. Magn Reson Med. 2001; 45:1030–1038. [PubMed: 11378881]
5. McGrath DM, Bradley DP, Tessier JL, Lacey T, Taylor CJ, Parker GJ. Comparison of model-based arterial input functions for dynamic contrast-enhanced MRI in tumor bearing rats. Magn Reson Med. 2009; 61:1173–1184. [PubMed: 19253360]
6. Tofts PS, Kermode AG. Measurement of the blood-brain barrier permeability and leakage space using dynamic MR imaging. 1. Fundamental concepts. Magn Reson Med. 1991; 17:357–367. [PubMed: 2062210]
7. Kovar DA, Lewis M, Karczmar GS. A new method for imaging perfusion and contrast extraction fraction: input functions derived from reference tissues. J Magn Reson Imaging. 1998; 8:1126–1134. [PubMed: 9786152]
8. Hansen AE, Pedersen H, Rostrup E, Larsson HB. Partial volume effect (PVE) on the arterial input function (AIF) in T1-weighted perfusion imaging and limitations of the multiplicative rescaling approach. Magn Reson Med. 2009; 62:1055–1059. [PubMed: 19672948]
9. Ivancevic MK, Zimine I, Montet X, Hyacinthe JN, Lazeyras F, Foxall D, Vallee JP. Inflow effect correction in fast gradient-echo perfusion imaging. Magn Reson Med. 2003; 50:885–891. [PubMed: 14586998]
10. Yang C, Karczmar GS, Medved M, Stadler WM. Estimating the arterial input function using two reference tissues in dynamic contrast-enhanced MRI studies: fundamental concepts and simulations. Magn Reson Med. 2004; 52:1110–1117. [PubMed: 15508148]
11. Yankeelov TE, Luci JJ, Lepage M, Li R, Debusk L, Lin PC, Price RR, Gore JC. Quantitative pharmacokinetic analysis of DCE-MRI data without an arterial input function: a reference region model. Magn Reson Imaging. 2005; 23:519–529. [PubMed: 15919597]
12. Yang C, Karczmar GS, Medved M, Stadler WM. Multiple reference tissue method for contrast agent arterial input function estimation. Magn Reson Med. 2007; 58:1266–1275. [PubMed: 17969061]
13. Medved M, Karczmar G, Yang C, Dignam J, Gajewski TF, Kindler H, Vokes E, MacEneany P, Mitchell MT, Stadler WM. Semiquantitative analysis of dynamic contrast enhanced MRI in cancer patients: Variability and changes in tumor tissue over time. J Magn Reson Imaging. 2004; 20:122–128. [PubMed: 15221817]
14. Joos KM, Blair WF, Brown TD, Gable RH. Flow field mapping in the anesthetized rat. Microsurgery. 1990; 11:12–18. [PubMed: 2139157]
15. McIntyre DJ, Ludwig C, Pasan A, Griffiths JR. A method for interleaved acquisition of a vascular input function for dynamic contrast-enhanced MRI in experimental rat tumours. NMR Biomed. 2004; 17:132–143. [PubMed: 15137038]
16. Fan X, Medved M, River JN, Zamora M, Corot C, Robert P, Bourrinet P, Lipton M, Culp RM, Karczmar GS. New model for analysis of dynamic contrast-enhanced MRI data distinguishes metastatic from nonmetastatic transplanted rodent prostate tumors. Magn Reson Med. 2004; 51:487–494. [PubMed: 15004789]
17. Weidensteiner C, Rausch M, McSheehy PM, Allegrini PR. Quantitative dynamic contrast-enhanced MRI in tumor-bearing rats and mice with inversion recovery TrueFISP and two contrast agents at 4.7 T. J Magn Reson Imaging. 2006; 24:646–656. [PubMed: 16878308]
18. Yankeelov TE, Cron GO, Addison CL, Wallace JC, Wilkins RC, Pappas BA, Santyr GE, Gore JC. Comparison of a reference region model with direct measurement of an AIF in the analysis of DCE-MRI data. Magn Reson Med. 2007; 57:353–361. [PubMed: 17260371]
19. Yankeelov TE, Rooney WD, Li X, Springer CS Jr. Variation of the relaxographic “shutter-speed” for transcytolemmal water exchange affects the CR bolus-tracking curve shape. Magn Reson Med. 2003; 50:1151–1169. [PubMed: 14648563]
20. Parker GJ, Roberts C, Macdonald A, Buonaccorsi GA, Cheung S, Buckley DL, Jackson A, Watson Y, Davies K, Jayson GC. Experimentally-derived functional form for a population-averaged high-temporal-resolution arterial input function for dynamic contrast-enhanced MRI. Magn Reson Med. 2006; 56:993–1000. [PubMed: 17036301]

21. Evelhoch JL. Key factors in the acquisition of contrast kinetic data for oncology. J Magn Reson Imaging. 1999; 10:254–259. [PubMed: 10508284]

22. Yankeelov TE, Rooney WD, Huang W, Dyke JP, Li X, Tudorica A, Lee JH, Koutcher JA, Springer CS Jr. Evidence for shutter-speed variation in CR bolus-tracking studies of human pathology. NMR Biomed. 2005; 18:173–185. [PubMed: 15578708]

23. Cheng HL. T1 measurement of flowing blood and arterial input function determination for quantitative 3D T1-weighted DCE-MRI. J Magn Reson Imaging. 2007; 25:1073–1078. [PubMed: 17410576]

24. Fan X, Karczmar GS. A new approach to analysis of the impulse response function (IRF) in dynamic contrast-enhanced MRI (DCEMRI): a simulation study. Magn Reson Med. 2009; 62:229–239. [PubMed: 19449381]

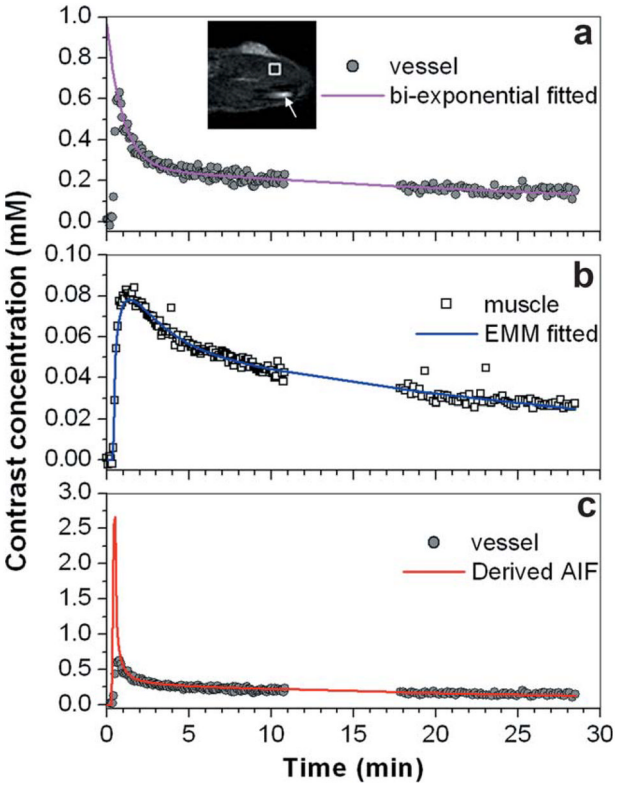

FIG. 1.

Illustration of the method used to estimate reference tissue K^{trans} and v_e: **(a)** A single pixel with an acceptable contrast media concentration vs. time curve (gray dots) was selected in a blood vessel (indicated by an arrow in the inset of image); the washout portion of the curve [$\hat{C}_p(t)$] was fitted with a bi-exponential function (purple line) and extrapolated back to zero from "t_{peak}." **b:** Contrast media concentration vs. time curve (open squares) in a muscle ROI (indicated by a square in the inset of image) was measured, and fitted with the EMM (blue line). **c:** The AIF was calculated from $C_m(t)$ in the reference tissue, based on the estimated K^{trans} and v_e (red line) and the contrast media concentration in the blood vessel [as in (a)] (gray dots). The difference image (post contrast media injection minus preinjection) is shown in the insert with an FOV of 2 cm × 2 cm.

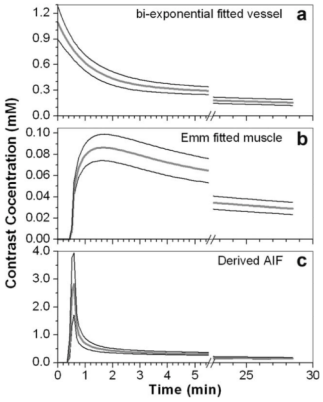

FIG. 2.

Averaged plot (thick gray line) over eight MRI experiments for: **(a)** the AIF measured in a blood vessel, fitted with the bi-exponential function; **(b)** $C_m(t)$ fitted with the EMM; and **(c)** AIF derived from reference tissue. The thin black lines indicate one standard deviation above and below the average for each time point.

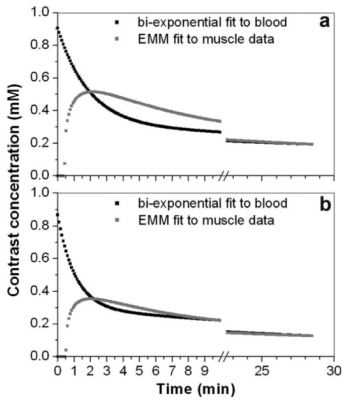

FIG. 3.

The plots of a bi-exponential fit to the plasma concentration of contrast media as a function of time, and $C_m(t)$ divided by v_e for **(a)** Case 2 and **(b)** Case 3 in Table 1. There was a large positive difference between the plasma and reference tissue concentrations of contrast media between ~30 s and ~1.5 min after bolus arrival, and a large negative difference between 1.5 minutes and ~7 minutes.

Table 1

Contrast Concentration Versus Time Curves From Vessels and for Muscle ROIs for Eight Selected MRI Experiments

Case	Bi-exponential fitted vessel curve [a_0, m_0; a_1, m_1]	EMM fitted muscle curve [A, q, α, β, γ]	K^{trans} (min^{-1})	v_e
1	[0.70, 1.04; 0.26, 0.024]	[0.12, 0.33, 0.94, 0.030, 0.46]	0.12	0.19
2	[0.59, 0.53; 0.31, 0.017]	[0.10, 0.32, 0.70, 0.021, 0.18]	0.05	0.15
3	[0.57, 0.94; 0.30, 0.030]	[0.13, 0.35, 1.02, 0.021, 0.17]	0.22	0.30
4	[1.00, 1.17; 0.31, 0.030]	[0.15, 0.49, 0.98, 0.031, 0.54]	0.18	0.23
5	[0.56, 0.67; 0.35, 0.020]	[0.15, 0.40, 1.12, 0.028, 0.59]	0.11	0.18
6	[0.90, 1.13; 0.32, 0.034]	[0.15, 0.49, 1.09, 0.037, 0.55]	0.21	0.21
7	[0.86, 0.96; 0.36, 0.033]	[0.10, 0.35, 1.02, 0.032, 0.46]	0.11	0.15
8	[0.87, 0.83; 0.42, 0.026]	[0.12, 0.33, 0.89, 0.028, 0.36]	0.08	0.14

The Bi-exponential fit for the AIF, the EMM parameters for $C_m(t)$, and estimated K^{trans} and v_e are given for each case. The Bi-exponential function was defined as $C_a(t) = a_0 \cdot \exp(-m_0 t) + a_1 \cdot \exp(-m_1 t)$, where a_0(mM) and m_0(min^{-1}) represent the fast component, and a_1(mM) and m_1(min^{-1}) represent the slow component. The EMM was defined as $C_m(t) = A \cdot (1-\exp(-\alpha t))^q \cdot \exp(-\beta t) \cdot (1 + \exp(-\gamma t))/2$, where A is in mM, q is unit-Less, and α, β, and γ is in min^{-1}